JOURNAL OF VIROLOGY, Mar. 2004, p. 3110–3122 Vol. 78, No. 6
0022-538X/04/$08.00+0 DOI: 10.1128/JVI.78.6.3110–3122.2004

Rapid Uncoating of Vector Genomes Is the Key to Efficient Liver Transduction with Pseudotyped Adeno-Associated Virus Vectors

Clare E. Thomas, Theresa A. Storm, Zan Huang, and Mark A. Kay*

Departments of Pediatrics and Genetics, Stanford University School of Medicine, Stanford, California 94305

Received 26 August 2003/Accepted 21 November 2003

Transduction of the liver with single-stranded adeno-associated virus serotype 2 (AAV2) vectors is inefficient; less than 10% of hepatocytes are permissive for stable transduction, and transgene expression is characterized by a lag phase of up to 6 weeks. AAV2-based vector genomes packaged inside AAV6 or AAV8 capsids can transduce the liver with higher efficiency, but the molecular mechanisms underlying this phenomenon have not been determined. We now show that the primary barrier to transduction of the liver with vectors based on AAV2 capsids is uncoating of vector genomes in the nucleus. The majority of AAV2 genomes persist as encapsidated single-stranded molecules within the nucleus for as long as 6 weeks after vector administration. Double-stranded vector genomes packaged inside AAV2 capsids are at least 50-fold more active than single-stranded counterparts, but these vectors also exhibit a lag phase before maximal gene expression. Vector genomes packaged inside AAV6 or AAV8 capsids do not persist as encapsidated molecules and are more biologically active than vector genomes packaged inside AAV2 capsids. Our data suggest that the rate of uncoating of vector genomes determines the ability of complementary plus and minus single-stranded genomes to anneal together and convert to stable, biologically active double-stranded molecular forms.

Adeno-associated virus (AAV) is one of the most promising virus systems under development for gene therapy. It is a small, nonpathogenic parvovirus that contains a linear single-stranded DNA (ssDNA) genome. Vectors derived from AAV are being evaluated in clinical trials for gene therapy of cystic fibrosis, hemophilia B, and muscular dystrophy, and so far the vectors appear to be safe (1, 2, 10, 14, 31).

Most AAV vectors in current use are derived from AAV serotype 2 (AAV2). AAV2 vectors can deliver genes to a wide variety of different cell types and tissues, but not all tissues are transduced efficiently. For gene transfer applications to the liver and the lung, high vector doses are required to obtain therapeutically relevant levels of transgene expression (23). It has become apparent that enhanced transduction of refractive tissues can be effected if the AAV2 vector genome (VG) is packaged inside capsids from alternative AAV2 serotypes, of which at least eight have been isolated to date (5, 9, 11, 27). Vectors based on AAV2 are being tested in a clinical trial of liver-directed gene transfer for hemophilia B, but recent studies suggest that vector pseudotypes composed of AAV2 VG packaged within AAV6 or AAV8 capsids are more efficient than AAV2 vectors at transducing the liver (9, 11). The mechanistic basis for increased liver transduction with alternative vector pseudotypes has not yet been established.

Studies in cell culture, purified nuclei, liver, and other tissues have identified several steps along the infection pathway for AAV2. AAV2 binds to cell surface heparin sulfate proteoglycan and is internalized into the cell via receptor-mediated endocytosis (3). After escaping the endosome, the virus traffics to a perinuclear compartment (3). How the virus genome enters the nucleus is more controversial. Hansen et al. (13) have reported that intact AAV2 capsids can bind and enter nuclei purified from 293 and NIH 3T3 cells and that the purified nuclei contain all of the factors necessary for virus uncoating. Fluorescently labeled AAV capsids have also been detected inside the nucleus after virus infection of cultured cells (28, 30). However, whether the majority of virus particles uncoat inside or outside the nucleus after infection of intact cells has remained open to debate (32).

After virus uncoating, the next step along the AAV transduction pathway is the conversion of the ss genome into a double-stranded (ds) molecular form. Studies in cell culture have shown that adenoviral gene products can promote de novo synthesis of the complementary strand (7, 8). In the liver, in the absence of coinfection with adenovirus, AAV VG conversion occurs through annealing of complementary plus and minus ss molecules, not by de novo synthesis of the second strand (22). This might be a general property of AAV vector transduction of other tissues besides the liver; a recent study showed that de novo second-strand synthesis was not required for AAV transduction of polarized epithelial cells (6).

Other studies have revealed further characteristics of the AAV2 transduction pathway in the liver: first, recombinant AAV (rAAV) VG can be detected in most hepatocyte nuclei within 24 h after vector administration, but less than 10% of these hepatocytes become stably transduced (18); second, the conversion of ss genomes to ds molecules occurs gradually, over a period of 6 weeks (18); thirdly, the monomeric linear ds genomes convert to a variety of ds molecular forms, including supercoiled ds circular monomers, circular and linear concatemers, and integrated proviral forms (20, 24).

In this study, we sought to define the major obstacles and rate-limiting steps to AAV2 transduction of the liver and to establish the mechanisms through which alternative vector pseudotypes mediate more efficient transduction of this organ. We investigated the following potential barriers to transduc-

* Corresponding author. Mailing address: Departments of Pediatrics and Genetics, 300 Pasteur Dr., Room G305A, Stanford University, Stanford, CA 94305. Phone: (650) 498-6531. Fax: (650) 498-6540. E-mail: markay@stanford.edu.

tion: translocation to the nucleus, uncoating of VG, and conversion of the ss AAV VG to the biologically active ds form. By comparing AAV2-based vectors with pseudotypes based on AAV6 and AAV8, we established that the primary barrier to AAV2 transduction of the liver is inefficient uncoating of VG in the nucleus.

MATERIALS AND METHODS

Construction of rAAV vectors. The construction and production of AAV2-hF.IX16 and AAV2-EF1α-nlsLacZ have been described elsewhere (19, 21). AAV2-hF.IX16 carried the hF.IX minigene (containing a 1.4-kb DNA fragment of the first intron from the hF.IX gene) and the bovine growth hormone polyadenylation signal [poly(A)], under the control of a liver-specific promoter (the apolipoprotein E hepatic locus control region human α1-antitrypsin [hAAT] gene promoter) (17). AAV2-EF1α-nlsLacZ carried the bacterial *lacZ* gene with a nuclear localization signal and the simian virus 40 (SV40) poly(A), under the control of the human elongation factor 1α (EF1α) promoter. VG were cross-packaged into capsids from AAV2, -6, or -8 as previously described (12), generating the following vector preparations: AAV2/2-hF.IX16, AAV2/6-hF.IX16, AAV2/8-hF.IX16, AAV2/2- (where 2/6 indicates that the AAV2 inverted terminal repeat [ITR]-flanked VG was packaged within a serotype 6 capsid). Vector particles were purified using cesium chloride gradient centrifugation, as previously described (4, 12). A second stock of AAV2/2-hF.IX16 was purified by heparin column chromatography. The physical particle titers were determined by a quantitative dot blot assay (15).

The vector AAV.luc was constructed as follows. A 262-bp DNA fragment containing a truncated version of the hAAT promoter (thAAT) fused to a 100-bp chimeric intron was excised from plasmid pAAV.F8.hAAT(intron) (29) using the restriction enzymes *Cla*I (blunted with mung bean nuclease) and *Mlu*I. This was ligated with plasmid pGL3-Basic (Promega), which had been digested with *Hin*dIII (blunted with mung bean nuclease) and *Mlu*I. The resulting construct (pGL3-thAAT-luc) contained the firefly luciferase gene and the SV40 poly(A), separated from the thAAT promoter by the 100-bp intron (see Fig. 8a). This expression cassette was amplified from pGL3-thAAT-luc using primers incorporating flanking *Not*I sites (forward [F] primer, TTA TTA GCG GCC GCG CTC TTA CGC GTG ACT CAG ATC CC; reverse [R] primer, TTA TAT GCG GCC GCG GCA TCG GTC GAC GGA TCC TTA TC) and was inserted into plasmid pAAV.EF1α.FIX (1), from which the hF.IX expression cassette had been removed by *Not*I digestion. The resulting plasmid was called pAAV.luc.

To construct the self-complementary (sc) vector scAAV.luc, pAAV.luc was digested with *Aat*II and *Xba*I and the fragment containing the right-hand ITR (upstream of the expression cassette) was inserted into pUC19. The resulting plasmid was digested with *Not*I and *Msc*I. Overhanging nucleotides were removed by digestion with mung bean nuclease, and the two blunt ends were ligated to recircularize the plasmid. The result was a deletion of 26 bp from the AAV ITR, incorporating the entirety of the D sequence, together with the terminal resolution sequence. The recircularized plasmid was digested with *Aat*II and *Xba*I, and the fragment containing the modified righthand ITR was cloned back into the pAAV.luc backbone, creating pscAAV.luc.

ssAAV.luc and scAAV.luc VG were each cross-packaged into AAV2 capsids as previously described (4), and vector particles were purified on cesium chloride gradients as above. After centrifugation, 0.5-ml fractions were collected through each gradient, and the refractive index of each fraction was measured. Five microliters of each fraction was electrophoresed on a 1% alkaline agarose gel, which was Southern blotted and hybridized with a vector-specific probe to determine which fractions contained the greatest proportion of sc or ss VG. Fractions with a refractive index of 1.3702 were collected for AAV.luc preparations (capsids contained an approximately 2.5-kb ss genome), whereas fractions containing the sc VG (approximately 4.9 kb) had a refractive index of 1.3736. Cesium chloride was removed by ultrafiltration-diafiltration as described previously (12), and the concentrations of ds vector particles (SCAAV.luc) and ss vector particles (AAV.luc) were determined by quantitative dot blot (15). The final yield of SCAAV.luc was approximately 10-fold lower than the yield of AAV.luc.

Animal procedures. Eight- to 10-week-old female C57BL/6 (for injection of AAV.hF.IX-16), female BALB/c (for injection of ssAAV.luc and scAAV.luc), and male C57BL/6 Rag-1 (for injection of AAV-EF1α-nlsLacZ) mice were purchased from the Jackson Laboratory (Bar Harbor, Maine). Injection of virus via the portal vein was performed as previously described (14, 19). Blood samples were collected from the retroorbital plexus. All animal procedures were performed according to the guidelines for animal care at Stanford University.

Protein analysis. hF.IX levels in mouse plasma were determined by an enzyme-linked immunosorbent assay (19). The detection limit of the assay was 2 ng/ml. β-Galactosidase expression was assessed by histological staining of 10-μm-thick frozen liver sections. Sections were fixed with 1.25% glutaraldehyde, stained with 5-bromo-4-chloro-3-indolylphosphate (X-Gal), and counterstained with light hematoxylin. Luciferase expression was measured in living animals. Mice were anesthetized intraperitoneally with ketamine (100 mg/kg of body weight) and xylazine (10 mg/kg). Ten minutes before imaging, an aqueous solution of luciferin (150 mg/kg; Xenogen, Alameda, Calif.) was injected intraperitoneally. Animals were placed into a light-tight chamber connected to a charge-coupled device camera system (IVIS; Xenogen), and photons emitted from luciferase-expressing cells and transmitted through the animals' bodies were quantified over a period of 10 min, using the software program Living Image (Xenogen).

Isolation of liver nuclei. Fresh mouse livers were minced on ice and homogenized in 12 ml of homogenization buffer (HB; 250 mM sucrose, 50 mM Tris-HCl [pH 7.5], 25 mM KCl, 5 mM $MgCl_2$, 0.5% NP-40, 1 mM phenylmethylsulfonyl fluoride [PMSF]), using a Dounce homogenizer. Nuclei and other organelles were collected by centrifugation for 10 min at 3,000 rpm in a Sorvall clinical centrifuge. The multilayered pellet was rehomogenized in 5 ml of HB, and the homogenate was filtered through six layers of surgical gauze into 40 ml of HB (without PMSF) in a 50-ml polypropylene tube. Nuclei were collected by centrifugation for 20 min at 1,500 rpm. The pellet was resuspended by gentle pipetting in 3 ml of HB (without PMSF) and was filtered through six layers of gauze, yielding a volume of approximately 1.5 ml. Three milliliters of high-density sucrose buffer (2.255 M sucrose, 50 mM Tris-HCl [pH 7.5], 25 mM KCl, 5 mM $MgCl_2$) was added to the suspension of nuclei and mixed to homogeneity by swirling. The suspension was then layered on top of a 4-ml cushion of sucrose buffer in a 12-ml UltraClear centrifuge tube (Beckman, Fullerton, Calif.). Nuclei were separated from contaminating organelles and plasma membrane sheets by centrifugation at 10,000 rpm in a Beckmann ultracentrifuge. The pelleted nuclei were resuspended in 400 μl of DNase I buffer (10 mM Tris-HCl [pH 7.5], 10 mM $MgCl_2$), divided into 100-μl aliquots, and stored at −80°C. All of the above procedures were performed in a cold room. Centrifugations were performed at 4°C. The purity of the isolated nuclei was assessed by light microscopy and by measuring levels of acid phosphatase contamination, using the EnzChek acid phosphatase assay (Molecular Probes, Inc., Eugene, Oreg.). The purity of the nuclei was consistently greater than 95%.

DNA analysis. Thawed nuclei (100 μl) were incubated with 200 μl of proteinase K buffer (final concentration, 10 mM Tris [pH 7.4], 10 mM $MgCl_2$, 10 mM EDTA, 0.6% sodium dodecyl sulfate [SDS], 2 mg of RNA-grade proteinase K [Invitrogen, Carlsbad, Calif.]/ml) for 2 h at 55°C. DNA was extracted once with phenol-chloroform and once with chloroform. The final aqueous phase was transferred to a clean tube and stored at −20°C. To assess the sensitivity of nuclear-localized AAV genomes to DNase I, a second aliquot of nuclei from each mouse was digested with 50 U of DNase I (10 U/μl; Roche, Basel, Switzerland) for 5 h, with occasional gentle vortexing, before digesting with proteinase K and extracting with phenol-chloroform and chloroform as described above.

AAV.hF.IX-16 VG were quantified in 10 ng of genomic DNA (extracted from nuclei that had not been digested with DNase I), or the same volume of DNase I-digested sample, by real-time PCR using the SYBR Green kit (PE Biosystems, Foster City, Calif.). Primers amplified a region within the intron segment of the hF.IX gene (F primer, CCT AAG CAC CCC CAG AAA GC; R primer, CGT CGA TTT CAC AGC TGA CAT C). Linearized plasmid DNA was used to generate the standard curve. The sensitivity of the assay was 0.006 vector copies per cell (10 copies per 10 ng of DNA). For each mouse, DNase I-digested and undigested samples were analyzed on the same 96-well plate. A control experiment was performed to assess whether VG were amplified with equal efficiency in samples that had been digested with DNase I versus undigested samples. Nuclei were isolated from naïve mice, as described above, and divided into halves. One half was digested with 50 U of DNase I as described above, while the other half was left undigested. Immediately before extracting with proteinase K and phenol-chloroform, samples were spiked with 10^7 ($n = 4$) or 10^8 ($n = 4$) VG of AAV.hF.IX-16. VG were quantified in 10 ng of genomic DNA (undigested), or the same volume of digested sample, as above. In both dose groups, detection of VG was 1.54-fold higher in samples that had been digested with DNase I, compared with their undigested counterparts. Values from digested samples were therefore normalized by dividing by 1.54. All undigested samples were also normalized for glyceraldehyde-3-phosphate dehydrogenase (GAPDH), using the rodent GAPDH Taqman kit (PE Biosystems).

Extraction of total genomic DNA from mouse livers and Southern blot analysis were performed as previously described (20). AAV.luc and SCAAV.luc genomes were quantified in 1 μg of genomic DNA extracted from whole mouse liver, using

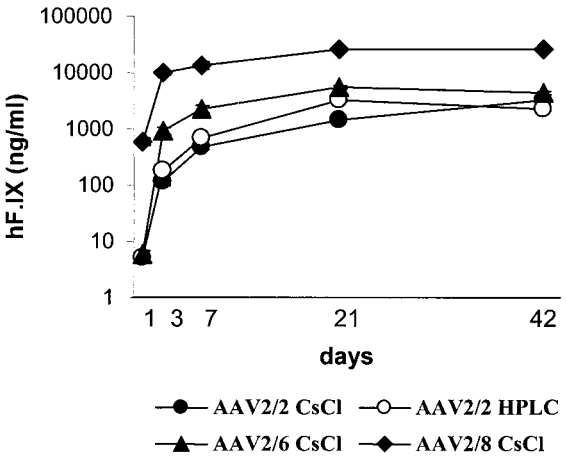

FIG. 1. Plasma hF.IX levels after intraportal administration of 10^{11} VG of AAV-hF.IX16 pseudotypes in C57BL/6 mice. The AAV pseudotypes contained an hF.IX expression cassette flanked by AAV2 ITRs packaged inside an AAV2 capsid (AAV2/2), an AAV6 capsid (AAV2/6), or an AAV8 capsid (AAV2/8). Vectors were purified by cesium chloride gradient centrifugation (CsCl) or heparin sulfate column chromatography (HPLC).

the SYBR Green real-time PCR kit with primer sets which amplified regions of the thAAT promoter (F, AGG TAA GTG CCG TGT GTG GTT; R, GCA CGC AAG GGC CAT AAC), the luciferase gene (F, AAC TGC CTG CGT GAG ATT CTC; R, CGC AGT ATC CGG AAT GAT TTG), and the SV40 poly(A) (F, GAC ATG ATA AGA TAC ATT GAT GAG TTT GG; R, GCA ATA GCA TCA CAA ATT TCA CAA AT). The sensitivity of the assay was 0.006 copies/cell (1,000 copies per μg of DNA). All samples were normalized for GAPDH, as described above.

Coimmunoprecipitation of AAV genomes from liver nuclei. Nuclei were isolated as described above, but the final pellet was resuspended in 3 ml of 10 mM Tris-HCl (pH 7.5), 10 mM $MgCl_2$, 20 mM NaCl, 1 mM PMSF, and divided into 1-ml aliquots in 1.5-ml microcentrifuge tubes. To reduce viscosity during subsequent solubilization, 50 U of DNase I (10 U/μl) was added to each tube and the nuclei were incubated at 37°C for 1 h. Detergent and EDTA were added to the following concentrations: 10 mM EDTA, 1% NP-40, 0.05% sodium deoxycholate, 0.1% SDS. All subsequent procedures were performed at 4°C. Solubilized nuclei were precleared with 50 μl of a 50% slurry of protein A-Sepharose beads (Sigma, St. Louis, Mo.) before incubating for 30 min with 50 μl of protein A-Sepharose beads preconjugated with 2 μl of either the A20 antibody, recognizing intact AAV2 capsids (American Research Products, Belmont, Mass.), or the anti-VP1,2,3 antibody, recognizing dissociated AAV2 capsid proteins (American Research Products), or with 50 μl of a 50% slurry of heparin-agarose beads (Sigma). Beads were pelleted by microcentrifugation and washed five times in 50 mM Tris-HCl (pH 7.5), 150 mM NaCl, 1% NP-40, 0.05% sodium deoxycholate, 0.1% SDS, before boiling for 5 min in 40 μl of alkaline gel loading buffer (50 mM NaOH, 1 mM EDTA, 25 mg of bromophenol blue/ml, 30 mg of Ficoll/ml). Twenty-five microliters of each sample was electrophoresed on a 1% alkaline agarose gel, which was subsequently Southern blotted and hybridized with a probe specific to the hF.IX expression cassette.

In vitro AAV uncoating assay. Nuclear and cytoplasmic extracts were prepared from mouse liver as follows. Fresh mouse livers were minced on ice and homogenized in 12 ml of homogenization buffer as described above. Nuclei and contaminating organelles were collected by centrifugation as above. Following the centrifugation, the supernatant (cytoplasmic extract) was filtered using a 45-μm-pore-size filter. The pellet was processed as described above to isolate the nuclei, which were subsequently solubilized by adding detergent to the following concentrations: 1% NP-40, 0.05% sodium deoxycholate, and 0.1% SDS. The protein concentrations in the nuclear and cytoplasmic extracts were measured using the Bio-Rad protein assay (Bio-Rad, Hercules, Calif.). To determine the effect of nuclear and cytoplasmic components on the sensitivity of purified AAV stocks to DNase I, 10^{10} particles of purified AAV2/2-hF.IX vector were incubated for 30 min at 37°C with 50 μg of nuclear extract, 50 μg of cytoplasmic extract, or buffer only (50 mM Tris-HCl [pH 7.5], 25 mM KCl, 5 mM $MgCl_2$) in a final volume of 200 μl, in a 1.5-ml tube ($n = 4$ per group). A cocktail of protease inhibitors was also added to each tube (Roche), and the final concentration of detergent in each sample was adjusted to 0.5% NP-40, 0.05% sodium deoxycholate, 0.05% SDS prior to the incubation. After incubation at 37°C, the concentration of $MgCl_2$ in each tube was adjusted to 10 mM, and 10 U of DNase I was added per tube. Samples were vortexed and incubated for a further hour at 37°C. EDTA was then added to a final concentration of 25 mM, and 20 μl of each sample was transferred to a fresh tube and boiled for 20 min. The denatured samples were diluted 10-fold with 1× Tris-EDTA, and DNase I-resistant VG in 5 μl were quantified by real-time PCR, using the SYBR Green kit with hF.IX-specific primers as described above. The remaining sample (unboiled) was analyzed by SDS-polyacrylamide gel electrophoresis and Western blotting with the anti-VP1,2,3 antibody (12) to assess whether the AAV capsid proteins had been degraded during the incubation with nuclear or cytoplasmic proteins.

RESULTS

Alternative AAV pseudotypes are more efficient at transducing the liver than AAV2/2. To investigate the comparative efficiencies of different AAV vector pseudotypes at transducing mouse liver, C57BL/6 mice were injected via the portal vein with 10^{11} VG of AAV2/2.hF.IX-16 ($n = 25$), AAV2/6.hF.IX-16 ($n = 20$), or AAV2/8.hF.IX-16 ($n = 25$). AAV2/2.hF.IX-16 comprised an AAV2 ITR-flanked hF.IX expression cassette packaged into an AAV2 capsid, and AAV2/6.hF.IX-16 and AAV2/8.hF.IX-16 vectors comprised the same AAV2 ITR-flanked VG, cross-packaged into AAV6 or AAV8 capsids, respectively. All three vectors were purified by cesium chloride gradient centrifugation. A fourth group of mice ($n = 20$) was injected with 10^{11} VG of AAV2/2.hF.IX-16 vector, which had been purified by high-performance liquid chromatography (HPLC). Four mice per group ($n = 20$ groups) or five mice per group ($n = 25$ groups) were sacrificed, and the livers were removed for subsequent analysis at 24 h, and 3, 7, 21, and 42 days post-vector injection. Blood was withdrawn from the retroorbital plexus prior to sacking for analysis of plasma hF.IX levels.

Plasma hF.IX levels rose slowly over 3 weeks after injection of HPLC-purified and cesium chloride-purified AAV2/2 vectors (Fig. 1). Maximal levels of expression from the AAV2/2 vectors were approximately 3,000 ng/ml (Fig. 1 and Table 1). Maximal plasma hF.IX levels from AAV2/6 and AAV2/8 vectors were approximately 2- and 10-fold higher than those with

TABLE 1. Hepatocyte transduction with AAV-EF1α-nlsLacZ (6 weeks postinjection)

Vector	Dose[a]	Mouse[b]	% Transduction[c]	Avg[d]
AAV2/2	3×10^{11}	1	3.0	3.4
		2	2.2	
		3	5.0	
AAV2/8	5×10^{10}	1	5.5	5.8
		2	6.7	
		3	5.2	
AAV2/8	3×10^{11}	1	16.0	13.1
		2	12.8	
		3	10.5	
AAV2/8	1.8×10^{12}	1	32.2	29.0
		2	19.8	
		3	35.0	

[a] VG injected per mouse.
[b] C57BL/6 Rag-1 mice.
[c] X-Gal-positive nuclei per total hepatocyte nuclei counted (at least 2,000 hepatocyte nuclei were counted per liver).
[d] Average percent transduction for the three mice.

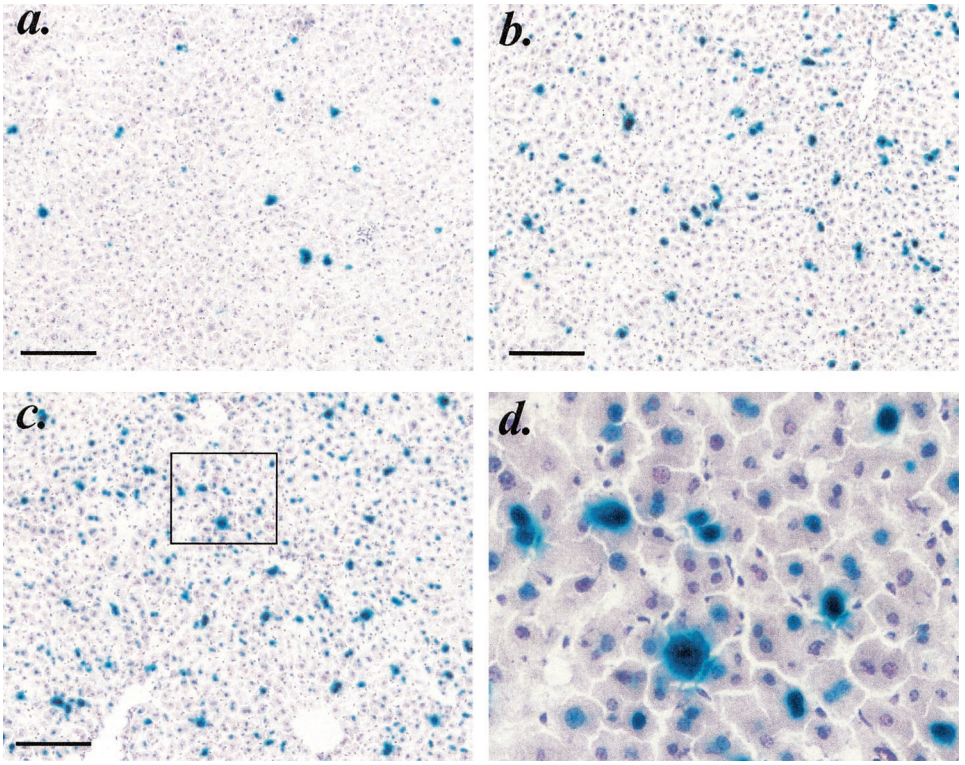

FIG. 2. X-Gal histochemistry of liver sections from immune-deficient C57BL/6 Rag-1 mice 6 weeks after intraportal delivery of *lacZ*-expressing vector pseudotypes. (a) Mice were injected with 3×10^{11} VG of AAV2/2-EF1α-nlslacZ. A section from a representative mouse is shown. (b and c) Sections from mice injected with 3×10^{11} VG (b) or 1.8×10^{12} VG (c) of AAV2/8-EF1α-nlslacZ. Scale bars in panels a to c represent 200 mm. (d) The boxed area in panel c.

the same dose of AAV2/2; however, high levels of expression from the pseudotyped vectors were achieved more rapidly than from AAV2/2 (Fig. 1 and Table 1). Therefore, at early time points, the difference in expression between the pseudotyped vectors and AAV2/2 was much greater. For example, at day 3, AAV2/6 expressed 5- to 8-fold higher levels and AAV2/8 expressed 54- to 84-fold higher levels than AAV2/2.

The AAV2/8 pseudotype transduces more than 10% of hepatocytes. It is well established that only a small subpopulation of hepatocytes is permissive to stable transduction with AAV2 vectors, even with high vector doses. Hepatocyte transduction with AAV2 increases linearly with increasing vector dose, up to a dose of 3×10^{11} VG per mouse, at which 3 to 5% of hepatocytes are stably transduced. Above this dose transduction with AAV2 starts to plateau, and maximum levels are reached at around 1.8×10^{12} VG, at which fewer than 10% of hepatocytes are transduced (23).

To investigate the relationship between vector dose and number of hepatocytes transduced using the AAV2/8 pseudotype, we injected C57BL/6 Rag-1 mice with 5×10^{10}, 3×10^{11}, or 1.8×10^{12} VG of AAV2/8.EF1α.nlsLacZ ($n = 3$ per group). For comparison, a fourth group of mice was injected with 3×10^{11} VG of AAV2/2.EF1α.nlsLacZ. Mice were sacrificed after 6 weeks, livers were sectioned and histologically stained, and the percentages of β-galactosidase-positive hepatocyte nuclei were scored for each group. Consistent with our previous observations, approximately 3% of hepatocytes were transduced with the AAV2/2 vector (Table 1 and Fig. 2). In contrast, nearly double this number of hepatocytes (5.8%) was transduced when sixfold fewer VG (5×10^{10}) were delivered inside AAV8 capsids (Table 1). Transduction with the AAV2/8 pseudotype increased approximately linearly over the three doses tested; each 6-fold increase in dose yielded a 2.2-fold increase in transduction. At the highest vector dose (1.8×10^{12} VG), nearly 30% of hepatocytes stably expressed β-galactosidase (Table 1 and Fig. 2).

Nuclear-localized VG delivered in AAV6 or AAV8 capsids are more biologically active than the same VG delivered in AAV2 capsids. As a first step to elucidate the basis for the enhanced efficiency of AAV2/6 and AAV2/8 vectors, we investigated whether the increased levels of transduction could be explained by a greater proportion of 2/6 and 2/8 VG within the nucleus (indicating more efficient trafficking to the nucleus). To our surprise, the levels of plasma hF.IX expressed by the different vectors did not correlate with the relative numbers of nuclear-localized VG. At day 3, the average number of nuclear-localized AAV2/2 VG per diploid genome equivalent (DGE) was 5.8 (CsCl-purified stock), yet an average of only 0.9 AAV2/6 VG per DGE was detected within the nucleus at this time point, even though plasma hF.IX levels in AAV2/6-injected animals were fivefold higher than those in AAV2/2 animals (Table 2). Furthermore, the average number of nuclear-localized AAV2/8 and AAV2/2 genomes per DGE was comparable at day 3 (4.63 for AAV2/8, compared with 5.8 for AAV2/2), yet plasma hF.IX levels in the AAV2/8-injected animals were 54-fold higher than the levels expressed from those

TABLE 2. Biological activity of nuclear-localized AAV VG

Vector (purification method)	Day	Nuclear-localized vector copies (VG/DGE)[a]	hFIX (ng/ml)[a]	VG activity[b]
AAV2/2 (HPLC)	1	4.03 ± 0.41	5.52 ± 0.2	<2
	3	3.90 ± 0.20	180 ± 13	46
	7	4.18 ± 0.53	694 ± 65	166
	21	3.78 ± 0.17	3,308 ± 302	875
	42	2.08 ± 0.09	2,188 ± 65	1,052
AAV2/2 (CsCl)	1	4.61 ± 0.41	0	0
	3	5.98 ± 0.20	116 ± 18	20
	7	4.19 ± 0.53	485 ± 32	116
	21	2.99 ± 0.17	1,451 ± 139	485
	42	2.58 ± 0.09	3,237 ± 119	1,255
AAV2/6 (CsCl)	1	0.96 ± 0.05	6.5 ± 1	7
	3	0.91 ± 0.08	935 ± 140	1,027
	7	0.84 ± 0.11	2,329 ± 358	2,773
	21	1.48 ± 0.17	5,627 ± 449	3,802
	42	1.53 ± 0.11	4,328 ± 275	2,828
AAV2/8 (CsCl)	1	2.99 ± 0.59	594 ± 90	198
	3	4.63 ± 0.677	9,739 ± 448	2,103
	7	6.90 ± 1.14	13,557 ± 2,314	1,964
	21	10.24 ± 2.05	25,738 ± 1,632	2,513
	42	8.56 ± 0.90	25,816 ± 519	3,015

[a] Values are means from four animals ± the standard error.
[b] Mean hFIX (in nanograms per milliliter) per mean nuclear-localized VG copy number (VG per DGE).

that received AAV2/2. Plasma hF.IX levels (in nanograms per milliliter) were divided by the average number of nuclear-localized VG per DGE to generate a measure of the average biological activity of the different VG at all the time points. As shown in Table 2, the average activity of the AAV2/2 (CsCl-purified) VG at day 3 was only 20 ng of hFIX/VG/DGE, compared with a value of 1,027 ng for AAV2/6 genomes and 2,103 ng for AAV2/8 genomes at the same time point.

Interestingly, the average activity of the nuclear-localized AAV2/2 genomes increased over time, parallel with a gradual net loss of genomes from the nucleus. In contrast, the average activity of the AAV2/6 and AAV2/8 genomes changed little over the time course, although the numbers of genomes gradually accumulated in the nucleus. Thus, the slow rise in plasma hF.IX in the AAV2/6- and AAV2/8-injected animals might be explained by slow trafficking of VG into the nucleus. This explanation is not sufficient to fully account for the slow rise in transgene expression in AAV2/2-injected animals, since the number of nuclear-localized AAV2/2 genomes declined over the 6-week time course.

Biological activity of nuclear-localized VG correlates with sensitivity to DNase I. Conversion of the ss AAV genome to a ds has been proposed as a rate-limiting step to transduction with AAV2 vectors. We have previously shown that conversion of AAV ssDNA to dsDNA occurs by annealing of cDNA strands in vivo (22). The ss VG packaged by AAV2, AAV6, or AAV8 capsids were identical in this study. We therefore hypothesized that the low average activity of VG delivered in AAV2 capsids, relative to those packaged in AAV6 or AAV8 capsids, was due to the failure of AAV2/2 to uncoat efficiently and release the ss genome. We rationalized that encapsidated VG would be resistant to digestion with DNase I and, accordingly, we assessed the sensitivity of the nuclear-localized VG to this enzyme.

As shown in Fig. 3, a high percentage of nuclear-localized AAV2/2 VG was resistant to DNase I throughout the time course of the study. More than 60% of the genomes resisted DNase I digestion up to 1 week after injection of the vector, and even at 6 weeks after vector injection (42 days) more than 30% of the nuclear-localized genomes remained resistant to DNase I. Nuclear-localized AAV2/6 genomes were more sensitive than AAV2/2 genomes to DNase I digestion. By 1 day after vector injection, only 30% of the nuclear-localized genomes were resistant to DNase I; this percentage dropped to 17% by day 3, and by 6 weeks post-vector injection only 4% of the AAV2/6 genomes remained DNase I resistant. Strikingly, AAV2/8 genomes were the most susceptible to DNase I digestion; at day 1, 3, and 42, the percentage of DNase I-resistant genomes was only around 10, 8, and 3%, respectively.

The relative sensitivities of the AAV2/2, AAV2/6, and AAV2/8 genomes to digestion with DNase I could be roughly correlated with their average biological activities. As previously discussed, at day 3 the average activities of the nuclear-localized AAV2/2, AAV2/6, and AAV2/8 genomes were 20 ng (only 36% were sensitive to DNase I), 1,027 ng (83% were DNase I sensitive), and 2,103 ng (92% were DNase sensitive) of hFIX/VG/DGE, respectively (Table 2).

Persistent DNase I-resistant AAV2/2 genomes in the nucleus are exclusively ss. To provide further support that the DNase I-resistant AAV2/2.hF.IX-16 genomes in the nucleus represented encapsidated genomes, we analyzed the molecular forms of all three vector species (AAV2/2, AAV2/6, and AAV2/8) 3 weeks after vector injection. Figure 4A shows a Southern blot of AAV VG extracted from purified nuclei, without predigestion with DNase I. A large proportion of the AAV2/2 genomes comigrated with a size marker for ss AAV. hF.IX-16 DNA, whereas ss AAV2/6 or AAV2/8 genomes were undetectable by Southern blotting (Fig. 4A). ds genome forms were absent in all samples extracted from nuclei that had been preincubated with DNase I but, strikingly, the ss AAV2/2.hF.IX-16 genomes remained intact after the DNase I digestion (Fig. 4B).

DNase I-resistant AAV2/2 genomes can be coimmunoprecipitated with an antibody recognizing intact capsids. To confirm that the DNase I-resistant ss AAV2/2 genomes were encapsidated, we attempted to coimmunoprecipitate VG from solubilized liver nuclei isolated 1, 3, or 7 days after injection of 5×10^{11} VG of AAV2/2.hF.IX-16, using an antibody that recognizes intact AAV capsids (A20). VG could be coimmunoprecipitated with the A20 antibody at all three time points (Fig. 5A); however, fewer genomes were recovered from nuclei isolated at 7 days post-vector injection than at the earlier time points, reflecting the decline of nuclear-localized AAV2/2 genomes over this time period (Fig. 5D). VG could also be recovered when heparin-Sepharose beads were used to capture the AAV2 capsids (Fig. 5B). In contrast, no VG were recovered when the anti-VP1,2,3 antibody was used, which recognizes dissociated capsid proteins but not intact capsids (Fig. 5C).

Close to 100% of AAV2-encapsidated VG become sensitive to DNase I after incubation with nuclear proteins in vitro. To rule out the possibility that a large fraction of AAV2/2.hF.IX-16 particles was defective for unpackaging (due to, perhaps, damage during purification of the vector particles), we performed an in vitro uncoating assay using purified AAV2/2.hF.

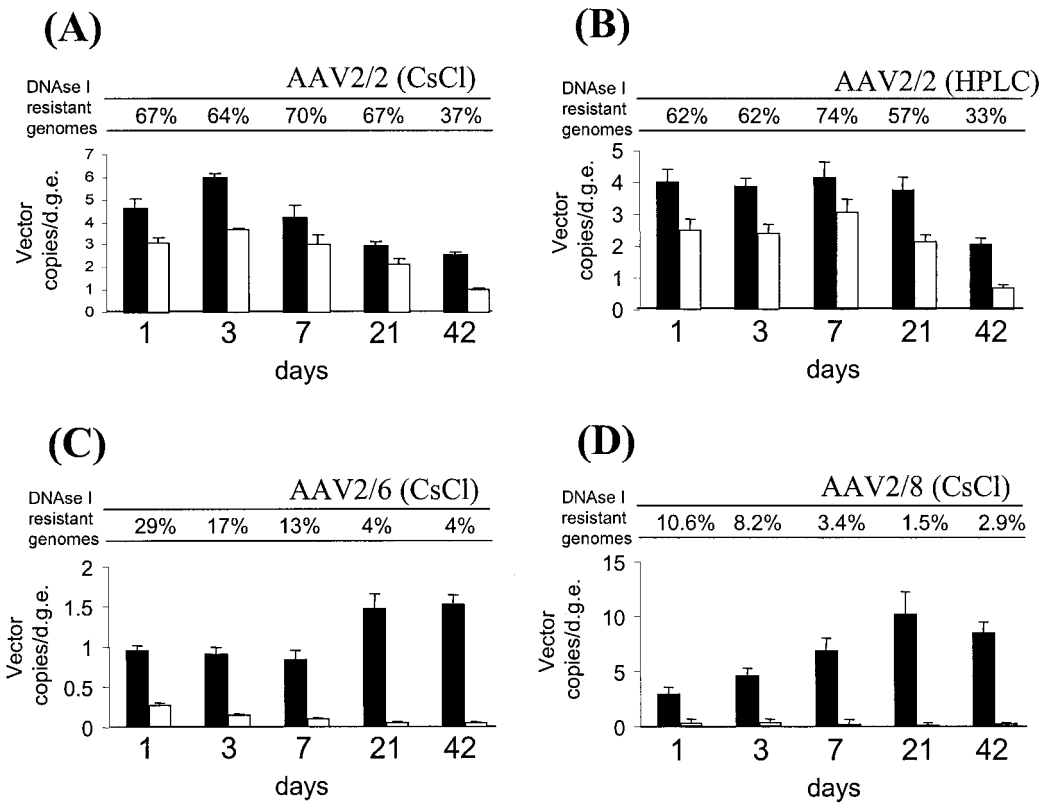

FIG. 3. Real-time PCR quantitation of the proportions of DNase I-resistant AAV genomes localized within the nucleus over time. Numbers of AAV genomes were quantified in total DNA extracted from purified liver nuclei prepared at different time points after intraportal injection of 10^{11} VG of pseudotyped AAV-hF.IX16 vectors into C57BL/6 mice. Solid black bars indicate the total number of nuclear-localized AAV genomes at each time point (expressed as copy numbers per DGE), and open bars indicate the relative number of DNase I-resistant AAV genomes. The ratio of DNase I-resistant to total nuclear-localized VG at each time point is expressed as a percentage above each graph. $n = 4$ mice per vector per time point. Error bars show standard errors of the means.

IX-16. Almost all of the purified vector particles could be rendered susceptible to DNase I following exposure to nuclear proteins in vitro (Fig. 6A). Incubation with cytoplasmic proteins resulted in a less pronounced destabilizing effect; more than 70% of the VG remained resistant to DNase I digestion. Analysis by SDS-polyacrylamide gel electrophoresis and Western blotting of the integrity of the AAV capsid proteins after incubation with the nuclear or cytoplasmic extracts indicated that the increase in susceptibility of the VG to DNase I had occurred through dissociation of capsid proteins and not through nonspecific protease degradation (Fig. 6B). These data support the hypothesis that uncoating of AAV VG occurs within the nucleus, and the data show that, theoretically, all of the AAV2/2 vector particles are amenable to uncoating.

AAV2/8 vector particles are not internalized more efficiently than AAV2/2 particles into liver, but a greater proportion of internalized AAV2/8 genomes persists within the liver. We next investigated the relative efficiencies of initial uptake of AAV2/2.hF.IX-16 and AAV2/8.hF.IX-16 particles in the liver. In this experiment, we looked at the total number of AAV VG in the liver, as opposed to the examination of nuclear-localized VG in our earlier experiments. Mice were injected with 10^{11} VG of vector and were sacrificed at 2 h ± 15 min ($n = 3$), 24 h ($n = 3$), and 6 weeks ($n = 4$) after vector injection. Genomic DNA was extracted from liver tissue, and AAV genomes were quantified by real-time PCR (Fig. 7). By 2 and 24 h after vector injection, there were more internalized AAV2/2 VG per DGE than AAV2/8 genomes. But a greater proportion of the AAV2/8 VG persisted in the liver; the difference between the number of VG at 6 weeks versus that at 2 h was much greater for AAV2/2hF.IX-16 than for the AAV2/8 pseudotype.

ds and ss VG packaged into AAV2 capsids both show a slow rise in transduction over time. Our previous data suggested that a large proportion of nuclear-localized AAV2/2.hF.IX-16 genomes persist for long periods of time encapsidated within the AAV2 protein shell. We hypothesized that slow uncoating of VG might contribute to the slow onset of expression seen from AAV2/2 (maximal levels of transgene expression are typically reached between 2 and 6 weeks after vector injection). Other groups have postulated that the slow rise in expression is due either to slow trafficking of AAV2 particles across the nuclear membrane or to slow conversion of ss AAV genomes to ds molecular forms. We have previously shown that in the liver, AAV genome conversion to a double strand occurs by annealing of two ss molecules, rather than by de novo synthesis of the complementary strand (22). One might imagine that annealing would occur rapidly, provided that both complementary strands were available at the same time.

sc AAV vectors, which package a ds AAV genome instead of an ss molecule, have recently been developed for gene transfer

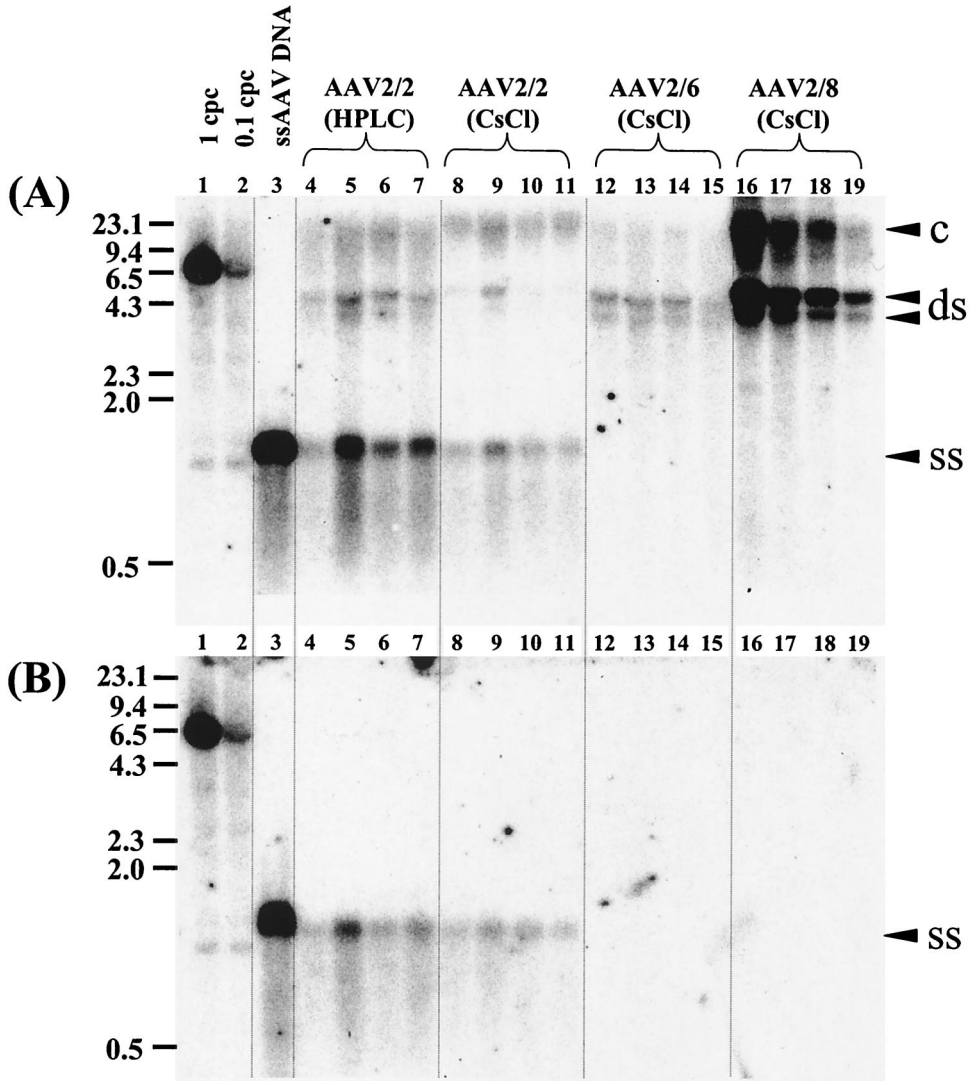

FIG. 4. Southern blot analysis of rAAV VG extracted from purified liver nuclei without preincubation with DNase I (A), or after incubation with DNase I for 5 h at 37°C (B). Vector forms in DNA samples extracted 3 weeks after injection of pseudotyped AAV-hF.IX16 vectors are shown. Forty micrograms of undigested total DNA (A) or the equivalent volume of DNase I-treated sample (B) was separated on a 1% agarose gel, blotted, and probed with a vector sequence-specific probe. Lanes 1 and 2, 1- and 0.1-VG/DGE standards, respectively (40 μg of DNA extracted from naïve mice was spiked with a 6.4-kb plasmid containing the AAVhF.IX16 sequence and then digested with *Sac*I prior to loading). A total of 10^7 VG of AAV-hF.IX16 extracted from purified vector stock was denatured by boiling for 5 min in the presence of formamide and loaded in lane 3 as a size marker for ss AAV-hF.IX genomes. Lanes 5 to 15 represent individual mice. Arrowheads indicate the different molecular forms of the AAV-hF.IX16 genome. ds indicates either relaxed circular, supercoiled circular, or linear ds forms. c, concatemers.

applications (16). If a single flanking AAV2 ITR is mutated to remove the terminal resolution sequence, this ITR is not nicked by the Rep protein during vector replication, and a hairpin genome structure is formed. If the mutated AAV VG is approximately half the length of a wild-type genome (2.4 kb, as opposed to 4.8 kb), the entire hairpin can be encapsidated. sc AAV2 vectors have been reported to mediate much more efficient transduction than ss AAV2 vectors in vitro and in vivo (16).

We predicted that if uncoating of ss AAV2/2 genomes were a rate-limiting step to liver transduction in vivo, then sc vectors should also be subject to slow uncoating and would also display a lag phase before maximal gene expression. To address this question, we constructed sc and ss vectors expressing the firefly luciferase gene, under the control of the liver-specific hAAT promoter. sc and ss VG were packaged into AAV2 capsids and were purified by cesium chloride gradient centrifugation (Fig. 8). BALB/c mice were injected with 5×10^9 VG of the sc vector (scAAV2/2.luc), 5×10^9 VG of the ss vector (ssAAV2/2.luc), or a 10-fold higher dose of ssAAV2/2.luc (5×10^{10} VG per mouse). Luciferase expression was measured over a time course lasting 1 year (Fig. 9).

By 4 days after vector injection, expression levels from the sc vector were 50-fold higher than from the same dose of ss vector and persisted with at least 50-fold-higher levels than the ss vector over the first 5 weeks of the study. Expression from scAAV.luc remained robust throughout the time course; by 16 weeks post-vector injection, expression from scAAV.luc had

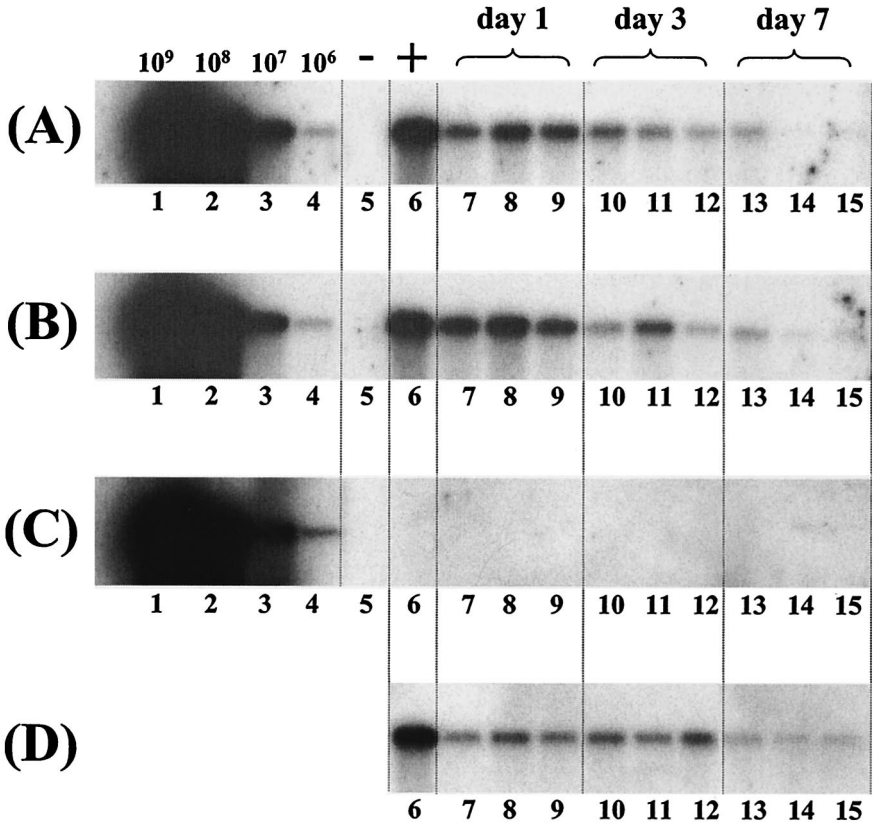

FIG. 5. Immunoprecipitation of intact AAV2/2 particles from purified liver nuclei. Liver nuclei purified at different time points after intraportal injection of 5×10^{11} VG of AAV2/2-hF.IX16 into C57BL/6 mice were incubated with DNase I for 1 h at 37°C. (A and B) Intact AAV capsids were immunoprecipitated from solubilized, DNase I-treated nuclei using the A20 antibody (A) or heparin-Sepharose beads (B). Immunoprecipitated capsids were boiled for 5 min in alkaline buffer, and the released VG were separated on a 1% alkaline agarose gel, blotted, and probed with a sequence-specific probe. (C) Control immunoprecipitations were performed with the anti-VP1,2,3 antibody, which recognizes dissociated, but not intact, capsid proteins. Positive and negative controls were performed for immunoprecipitations with all antibodies. For the positive control, purified nuclei were spiked with 10^9 VG of AAV2/2-hF.IX.16 prior to solubilization (lane 6). For the negative control, solubilized nuclei were spiked with 10^{10} VG of AAV-hF.IX16 DNA extracted from purified AAV2/2-hF.IX16 particles (lane 5). Lanes 1 to 4 show copy number standards (purified AAV2/2-hF.IX particles boiled in alkaline buffer prior to loading). Lanes 7 to 15 represent individual mice. (D) Ten microliters of supernatant from solubilized nuclei (from a total volume of 1 ml for each mouse) removed prior to immunoprecipitation was also boiled in alkaline buffer and loaded on a gel.

dropped slightly but was still 43-fold higher than from the same dose of ss vector, and by 1 year after injection of the vector scAAV.luc it was still generating 20-fold higher levels of luciferase expression than its ss counterpart (Fig. 9A and 10C). Although the scAAV2/2.luc vector was dramatically more efficient than the ss vector, both sc and ss vectors showed similar kinetics of transgene expression: levels of luciferase expression slowly increased over the first 5 weeks after vector injection (Fig. 9B to D).

sc VG are more stable than ss VG. Animals injected with scAAV2/2.luc and ssAAV2/2.luc vectors were sacrificed at 1 year post-vector administration. VG in genomic DNA extracted from liver tissue were quantified by real-time PCR, using three separate sets of primers which amplified regions within the promoter, the transgene, or the vector poly(A) (Fig. 10A). No vector-specific amplification could be detected in animals injected with either 5×10^9 VG of the ss vector or in those that had been injected with the 10-fold higher dose of 5×10^{10} VG (Fig. 10B), although these animals were expressing luciferase at this time point (Fig. 10C). Thus, the number of VG in these animals was fewer than 0.006 VG per DGE (which was the sensitivity threshold of our assay). In contrast, VG were detected in both of the animals which had been injected with just 5×10^9 VG of the sc vector (Fig. 10B). The results using all three primer sets were similar: average vector copy numbers for the two mice in this group were 0.05 and 0.024 VG/DGE. These data indicate that sc VG are retained more efficiently within the hepatocyte than the same dose of ss VG.

DISCUSSION

The aim of this study was to determine why AAV6 and AAV8 pseudotyped vectors mediate more efficient transduction of the liver than vectors based on AAV2. Our findings have led us to construct a model for AAV vector transduction of the liver, which we would like to propose here.

The crux of our model (Fig. 11) is that the rate of uncoating of VG determines the ability of complementary plus and minus ss genomes to convert to stable and biologically active ds molecular forms. We suggest that ss VG are only stable when packaged within the AAV capsid shell; when these genomes

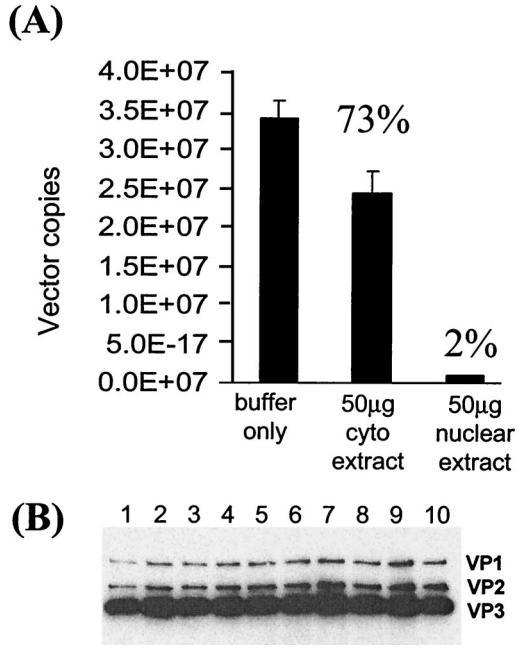

FIG. 6. Real-time PCR quantitation of DNase I-resistant genomes after incubation with nuclear extract or cytoplasmic extract. A total of 10^{10} particles of purified AAV2/2-hF.IX vector were incubated for 30 min at 37°C with 50 μg of nuclear extract, cytoplasmic extract, or the same volume of buffer alone, before digesting with DNase I for a further hour at 37°C (final volume, 100 μl). (A) DNase I-resistant VG in 5 μl were quantified by real-time PCR. Error bars show the standard error of the mean of four samples per group. (B) Twenty microliters of the remaining sample was analyzed by Western blotting with the anti-VP1,2,3 antibody to detect the integrity of the capsid proteins following incubation with nuclear or cytoplasmic extract. Lanes 1 and 2, AAV particles incubated with buffer only; lanes 3 to 6, AAV particles incubated with cytoplasmic extract; lanes 7 to 10, AAV particles incubated with nuclear extract.

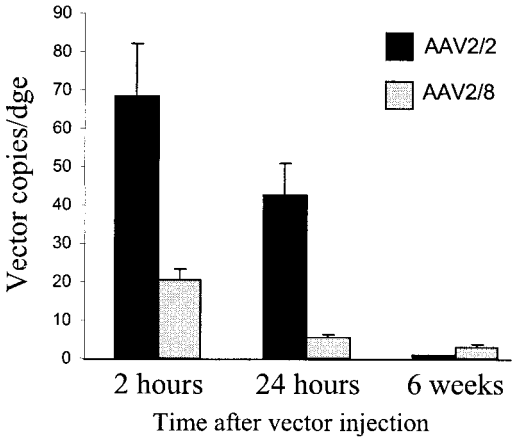

FIG. 7. Real-time PCR quantitation of AAV genomes present in genomic DNA extracted from liver tissue. C57BL/6 mice were injected with 10^{11} VG of AAV2/2.hF.IX-16 or AAV2/8.hF.IX-16, and livers were harvested 2 or 24 h or 6 weeks after vector injection.

are released they are rapidly degraded, unless they become stabilized as ds molecules. We believe that in the liver this occurs primarily by annealing of complementary ss AAV genomes (22), although others have proposed that, at least in cultured cells, the second strand is synthesized (7, 8).

In our model, slow uncoating effectively limits the concentration of naked ss genomes available for annealing, so most of the AAV genomes become degraded after release. We propose that VG packaged within AAV2 capsids fail to uncoat efficiently and, therefore, only a small fraction of the genomes that enter the nucleus anneal and form stable ds molecules; the rest are lost.

Consistent with this model, we observed experimentally that a large proportion of nuclear-localized AAV2/2 genomes persisted as encapsidated ss genomes for as long as 6 weeks after the vector injection. Furthermore, the average biological activity of nuclear-localized AAV2/2 genomes was low at early time points after vector injection, but this average activity increased over 6 weeks, parallel with a net loss of VG from the nucleus. sc AAV2/2 genomes persisted to a greater extent than ss genomes, supporting the hypothesis that naked ss genomes are unstable.

Our experiments suggest that the slow rise in gene expression typical of transduction with AAV2 vectors is, at least in part, due to the slow uncoating of VG. Slow trafficking to the nucleus might also contribute to the lag phase but, importantly, our data suggest that in the liver, the conversion of uncoated ss AAV VG to ds forms is not in itself a rate-limiting step; sc vectors exhibited a slow rise in gene expression, as well as ss vectors, although the absolute levels of transgene expression from sc vectors were much higher at all time points. The fact that sc VG are more biologically active than ss genomes and therefore produce much more transgene product at early time points may explain why McCarty et al. (16) reported that an sc AAV vector expressing erythropoietin (EPO) resulted in more rapid elevation of hematocrit than an ss vector. In their system, McCarty and colleagues did not measure the rise in transgene expression directly; instead, they measured the effect of the transgene product. Hematocrit elevation would not occur until a threshold of EPO expression had been reached, which would

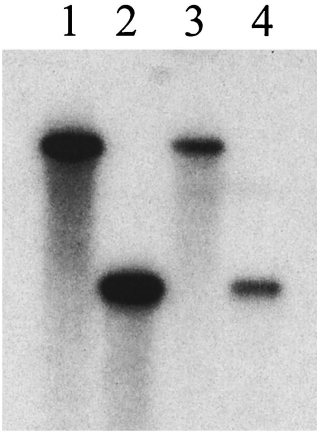

FIG. 8. Purity of sc (lane 3) and ss (lane 4) AAV.luc vectors after cesium chloride gradient fractionation. Aliquots of cesium chloride gradient fractions containing sc AAV.luc (refractive index, 1.3736) or ss AAV.luc (refractive index, 1.3702) were electrophoresed on a 1% alkaline agarose gel, Southern blotted, and hybridized with a vector-specific probe. The sc genome migrated with the 4.8-kb marker (lane 1), whereas the ss genome migrated with the 2.4-kb marker (lane 2).

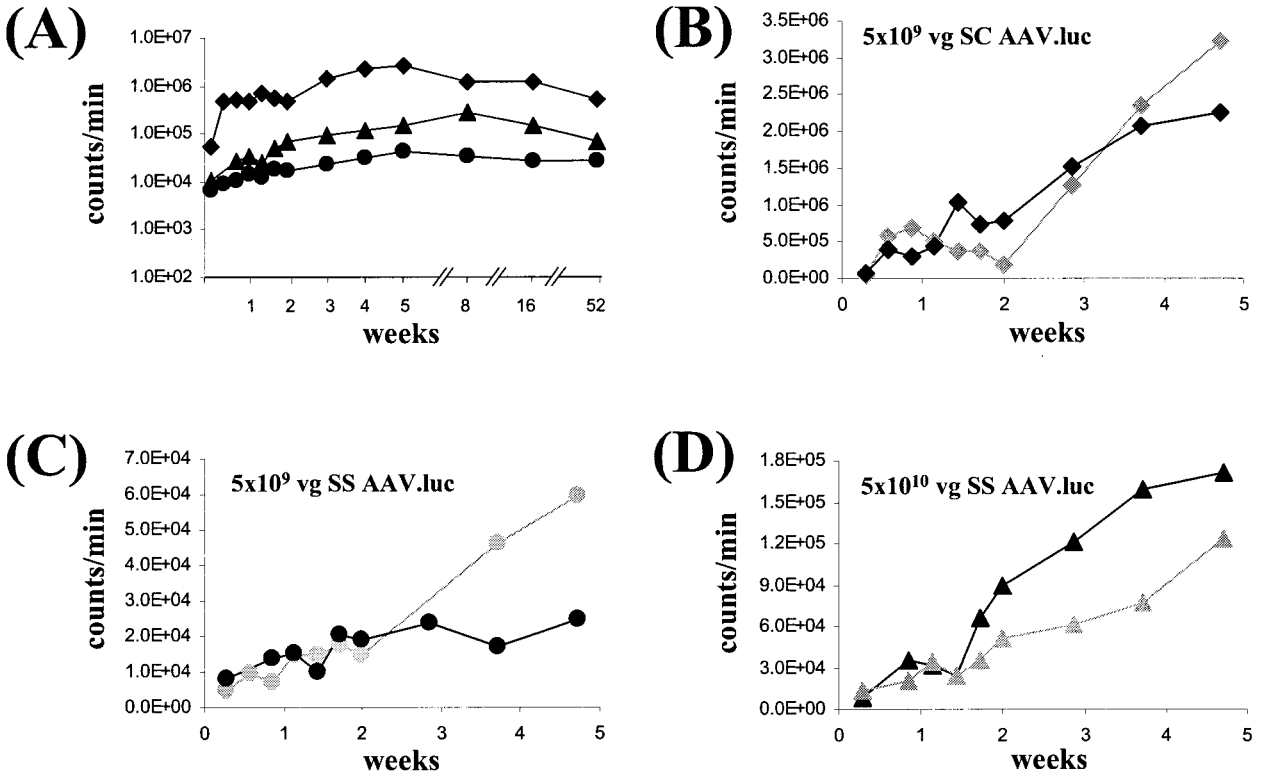

FIG. 9. A time course of expression from sc versus ss AAV2/2 vectors expressing luciferase. BALB/c mice ($n = 2$ per virus) were injected with 5×10^9 VG of sc AAV2/2.luc (■), 5×10^{10} VG of ss AAV2/2.luc (▲), or 5×10^9 VG of ss AAV2/2.luc (●). (A) Mean luciferase expression for all three virus groups plotted on a log scale. Luciferase expression from the sc vector was up to 50-fold higher than luciferase expression from the same dose of ss vector and remained high over the 1-year period of study. (B to D) Luciferase expression from sc vectors as well as ss vectors gradually increased over the first 5 weeks after vector injection. The expression profiles for two individual animals per virus dose are shown.

be reached earlier by the more biologically active sc vector. Likewise, an upper threshold of EPO presumably exists, above which no further elevation of hematocrit is possible. Thus, expression from the sc vector might falsely appear to plateau shortly after vector administration.

We suggest that while slow uncoating leads to the majority of VG being degraded, rapid capsid disassembly enhances the probability of genome stabilization by annealing (Fig. 11). Experimentally, we observed that almost all the nuclear-localized genomes delivered in AAV8 capsids were sensitive to DNase I, even at early time points, indicating that they were not encapsidated. Furthermore, the average biological activity of these genomes was high at early time points and did not substantially increase over 6 weeks. The net number of nuclear-localized AAV2/8 genomes increased over time, indicating that the vector particles trafficked slowly to the nucleus and that the genomes persisted within the nucleus. Thus, we propose that AAV8 capsids disassemble rapidly upon entry into the nucleus, allowing efficient annealing and stabilization of the ss AAV DNA.

Our data suggest that the basis for the increased liver transduction mediated by alternative vector pseudotypes is more rapid uncoating of VG in the nucleus (facilitating more-efficient annealing of VG). A pertinent question is why the AAV2 capsid disassembles less efficiently than the AAV6 or AAV8 capsids. Our in vitro data suggest that all AAV2/2 vector particles can, in principle, be uncoated very efficiently by nuclear factors. It therefore seems most likely that uncoating takes place within a particular nuclear compartment and that AAV2 capsids fail to traffic efficiently to this compartment. Muzyczka and colleagues investigated trafficking of AAV2 in HeLa cells and found that AAV particles quickly surrounded the HeLa cell nucleus, but they translocated slowly across the nuclear membrane (32). These researchers detected little intact capsid within the interior of the nucleus and concluded that uncoating occurred before, or during, nuclear entry. (Interestingly, these authors found that coinfection of HeLa cells with adenovirus accelerated translocation across the nuclear membrane and, in this case, intact capsids could readily be detected within the nucleus.) Our data indicate that, in the hepatocyte, uncoating is mediated by nuclear factors, but otherwise our results support the conclusions of Muzyczka and colleagues, that inefficient trafficking of AAV2 is a major obstacle to transduction.

The pathway used by AAV to access the interior of the nucleus has not yet been established. Intriguingly, experiments from two groups have indicated that the AAV vector particle does not use the nuclear pore complex as its entry portal (13, 32). It is difficult to envisage alternative routes of entry that might be used by AAV but, clearly, we understand little about how this virus traffics across the nuclear membrane. One possible explanation of our data is that in the absence of adenovirus infection, AAV2 particles become trapped within the nuclear membrane and slowly escape to the interior of the

(A)

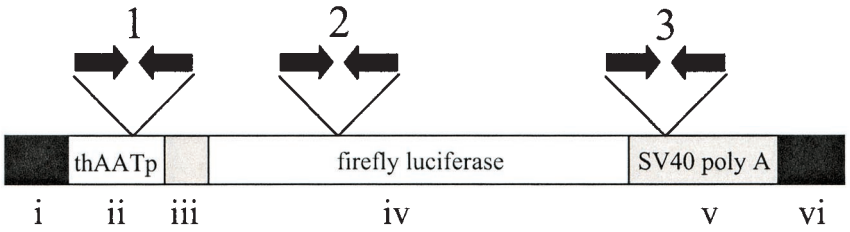

(B)

Vector	Dose (vg/mouse)	Mouse	Vector copies/dge 1[a]	2[b]	3[c]
Single-stranded	$5x10^9$	1*	<0.006[d]	<0.006	<0.006
Single-stranded	$5x10^{10}$	1	<0.006	<0.006	<0.006
		2	<0.006	<0.006	<0.006
Self-complementary	$5x10^9$	1	0.040	0.072	0.043
		2	0.020	0.024	0.028

[a,b,c] primers annealing within hAAT promoter[a], luciferase gene[b], or SV40 polyA[c].
[d] assay sensitivity threshold was 0.006 vg/dge.

(C)

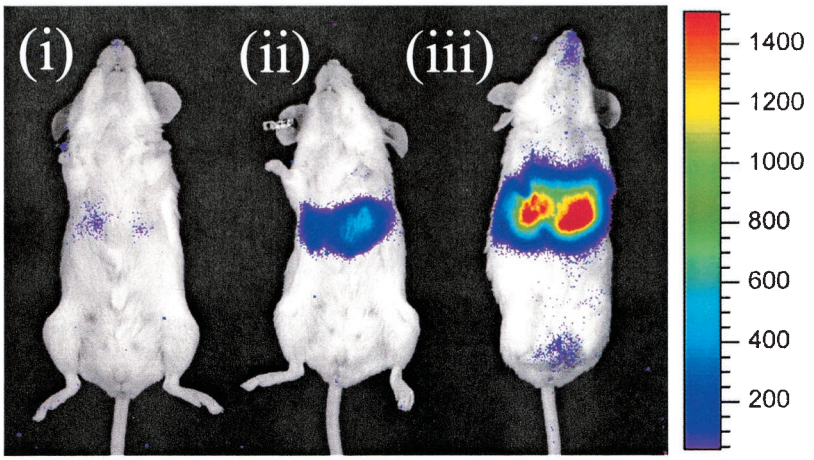

FIG. 10. Real-time PCR quantitation of sc and ss AAV.luc genomes in genomic DNA extracted from the livers of BALB/c mice 1 year after vector injection. (A) sc or ss AAV.luc VG were quantified using three sets of primer-probe combinations. ss VG were undetectable in mice that had been injected with 5×10^9 or 5×10^{10} VG. (B) In contrast, sc VG were reproducibly detected with all three primer-probe sets, even though only the low dose of 5×10^9 VG had been injected. (C) Luciferase expression in three representative mice 1 year after vector injection. (i) Mouse injected with 5×10^9 VG of ss AAV.luv; (ii) mouse injected with 5×10^{10} VG of ss AAV.luc; (iii) mouse injected with 5×10^9 VG of SC AAV.luc. One of the mice in the group injected with 5×10^9 VG of the ss vector died before the 1-year time point.

nucleus, where they are disassembled. AAV6 and AAV8 particles might cross the membrane barrier more rapidly.

A hallmark of AAV2 transduction of the liver is that only a small subpopulation of hepatocytes (less than 10%) is permissible to stable transduction (23, 33). As a first interpretation, this would appear to suggest that annealing of complementary ss genomes might be inhibited in 90% of hepatocytes; sc vectors might be able to transduce more cells because they are already ds molecules. As seen in this and a previous study (9), AAV8 capsids packaging ss VG are also able to overcome the 10% limit.

An explanation for why both ss AAV8 vectors and sc AAV2 vectors could transduce more hepatocytes than ss AAV2 vectors is suggested by our model (Fig. 11). It has been proposed that cellular factors exist that bind to the ends of the AAV genome and inhibit second-strand synthesis. One such protein is the immunophilin FKBP52 (25, 26). Binding of cellular proteins to ss VG could also obstruct annealing and might feasibly

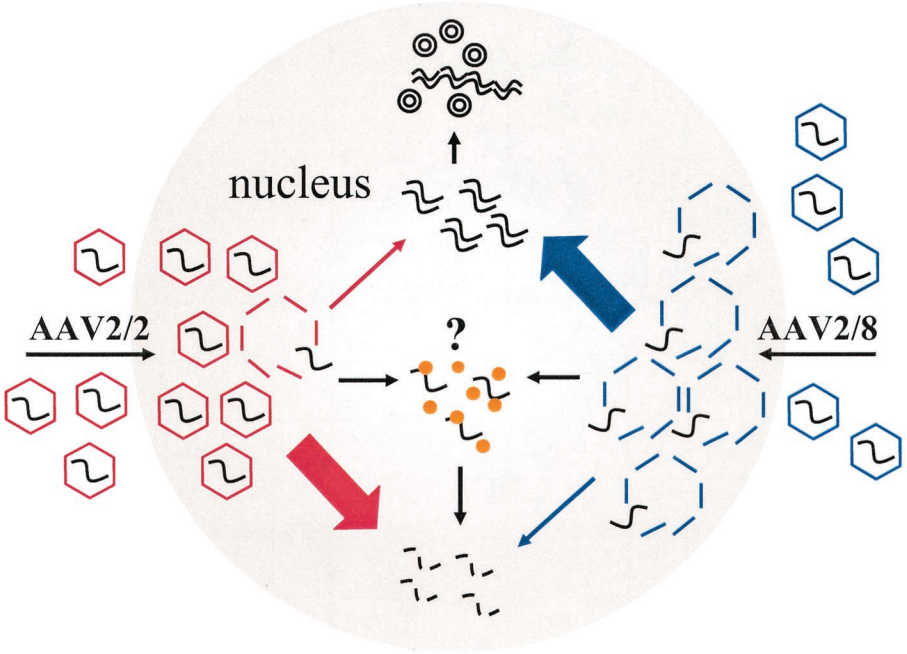

FIG. 11. Theoretical model for rAAV transduction of the liver. AAV2 VG packaged within an AAV2 shell (AAV2/2) traffic slowly to the nucleus. Capsid disassembly is mediated by a nuclear factor(s). Upon uncoating, ss VG either become stabilized by annealing rapidly with complementary AAV genomes or they are degraded and lost. The rate of uncoating determines the proportion of VG that become stabilized by annealing or lost by degradation. The AAV2/2 pseudotype uncoats slowly. Annealing is therefore inefficient, and most of the VG are removed by degradation. A nuclear protein (such as FKBP52) might bind to the ss AAV genomes and physically obstruct annealing or target the genome for degradation. The AAV2/8 pseudotype, containing the AAV2 genome packaged within an AAV2/8 capsid, is more efficient than the AAV2/2 pseudotype because it uncoats rapidly. Annealing of complementary genomes occurs with higher efficiency, and a reduced proportion of VG are lost by degradation. Thus, AAV2/8 vectors mediate more efficient liver transduction than AAV2/2 vectors.

target the single strands for destruction. According to our model, the ss genome has one of two fates: either it anneals with another genome to form a stable, active molecule, or it is targeted by a cellular protein (a candidate being FKBP52), which targets it for degradation. We have suggested that annealing occurs rapidly, as soon as the VG are uncoated (provided a complementary strand is available within the same microenvironment). Thus, AAV8 VG, which are uncoated efficiently, are more likely to be processed along the annealing pathway than along the pathway that leads to degradation. sc genomes are already ds and are therefore already stable. Conversely, AAV2 VG, which are released gradually, are most likely to bind with the inhibitory protein and become degraded. The 10% of hepatocytes that are permissive to transduction with ss AAV2 vectors might lack the inhibitory cellular protein. Alternatively, trafficking to the compartment in which uncoating takes place may only occur efficiently in 10% of hepatocytes.

Many aspects of our model are speculative and have yet to be tested experimentally. Furthermore, multiple barriers to AAV2 transduction exist that are outside the boundaries of the model. For example, other studies have demonstrated that many vector particles are targeted for proteasome degradation before reaching the cell nucleus (6, 34). Whether the capsids of different AAV serotypes are equally susceptible to proteasome degradation remains to be determined. Other events occurring inside the nucleus might also affect levels of transduction. Nakai et al. (24) have shown that different ds molecular forms have different capacities for transgene expression. It is not clear how quickly linear ds molecules convert to supercoiled circular forms or concatemers, but it is feasible that these conversions could contribute to the slow rise in transgene expression. Nonetheless, our present study provides a mechanistic basis for the enhanced efficiency of pseudotyped AAV vectors and supports the use of alternative AAV capsids for liver-directed gene therapy.

ACKNOWLEDGMENTS

This work was supported by NIH grants HL64274 and HL66948 (M.A.K.).

REFERENCES

1. **Aitken, M. L., R. B. Moss, D. A. Waltz, M. E. Dovey, M. R. Tonelli, S. C. McNamara, R. L. Gibson, B. W. Ramsey, B. J. Carter, and T. C. Reynolds.** 2001. A phase I study of aerosolized administration of tgAAVCF to cystic fibrosis subjects with mild lung disease. Hum. Gene Ther. **12:**1907–1916.
2. **Arruda, V. R., P. A. Fields, R. Milner, L. Wainwright, M. P. De Miguel, P. J. Donovan, R. W. Herzog, T. C. Nichols, J. A. Biegel, M. Razavi, M. Dake, D. Huff, A. W. Flake, L. Couto, M. A. Kay, and K. High.** 2001. Lack of germline transmission of vector sequences following systemic administration of recombinant AAV-2 vector in males. Mol. Ther. **4:**586–592.
3. **Bartlett, J. S., R. Wilcher, and R. J. Samulski.** 2000. Infectious entry pathway of adeno-associated virus and adeno-associated virus vectors. J. Virol. **74:** 2777–2785.
4. **Burton, M., H. Nakai, P. Colosi, J. Cunningham, R. Mitchell, and L. Couto.** 1999. Coexpression of factor VIII heavy and light chain adeno-associated viral vectors produces biologically active protein. Proc. Natl. Acad. Sci. USA **96:**12725–12730.
5. **Chao, H., Y. Liu, J. Rabinowitz, C. Li, R. J. Samulski, and C. E. Walsh.** 2000. Several log increase in therapeutic transgene delivery by distinct adeno-associated viral serotype vectors. Mol. Ther. **2:**619–623.

6. **Ding, W., Z. Yan, R. Zak, M. Saavedra, D. M. Rodman, and J. F. Engelhardt.** 2003. Second-strand genome conversion of adeno-associated virus type 2 (AAV-2) and AAV-5 is not rate limiting following apical infection of polarized human airway epithelia. J. Virol. **77:**7361–7366.
7. **Ferrari, F. K., T. Samulski, T. Shenk, and R. J. Samulski.** 1996. Second-strand synthesis is a rate-limiting step for efficient transduction by recombinant adeno-associated virus vectors. J. Virol. **70:**3227–3234.
8. **Fisher, K. J., G. P. Gao, M. D. Weitzman, R. DeMatteo, J. F. Burda, and J. M. Wilson.** 1996. Transduction with recombinant adeno-associated virus for gene therapy is limited by leading-strand synthesis. J. Virol. **70:**520–532.
9. **Gao, G. P., M. R. Alvira, L. Wang, R. Calcedo, J. Johnston, and J. M. Wilson.** 2002. Novel adeno-associated viruses from rhesus monkeys as vectors for human gene therapy. Proc. Natl. Acad. Sci. USA **99:**11854–11859.
10. **Greelish, J. P., L. T. Su, E. B. Lankford, J. M. Burkman, H. Chen, S. K. Konig, I. M. Mercier, P. R. Desjardins, M. A. Mitchell, X. G. Zheng, J. Leferovich, G. P. Gao, R. J. Balice-Gordon, J. M. Wilson, and H. H. Stedman.** 1999. Stable restoration of the sarcoglycan complex in dystrophic muscle perfused with histamine and a recombinant adeno-associated viral vector. Nat. Med. **5:**439–443.
11. **Grimm, D., and M. A. Kay.** 2003. From virus evolution to vector revolution: use of naturally occurring serotypes of adeno-associated virus (AAV) as novel vectors for human gene therapy. Curr. Gene Ther. **3:**281–304.
12. **Grimm, D., S. Zhou, H. Nakai, C. E. Thomas, T. A. Storm, S. Fuess, T. Matsushita, J. Allen, R. Surosky, M. Lochrie, L. Meuse, A. McClelland, P. Colosi, and M. A. Kay.** 2003. Preclinical in vivo evaluation of pseudotyped adeno-associated virus vectors for liver gene therapy. Blood **102:**2412–2419
13. **Hansen, J., K. Qing, and A. Srivastava.** 2001. Infection of purified nuclei by adeno-associated virus 2. Mol. Ther. **4:**289–296.
14. **Kay, M. A., Q. Li, T. J. Liu, F. Leland, C. Toman, M. Finegold, and S. L. Woo.** 1992. Hepatic gene therapy: persistent expression of human a1-antitrypsin in mice after direct gene delivery *in vivo.* Hum. Gene Ther. **3:**641–647.
15. **Kessler, P. D., G. M. Podsakoff, X. Chen, S. A. McQuiston, P. C. Colosi, L. A. Matelis, G. J. Jurtzman, and B. J. Byrne.** 1996. Gene delivery to skeletal muscle results in sustained expression and systemic delivery of a therapeutic protein. Proc. Natl. Acad. Sci. USA **93:**14082–14087.
16. **McCarty, D. M., P. E. Monahan, and R. J. Samulski.** 2001. Self-complementary recombinant adeno-associated virus (scAAV) vectors promote efficient transduction independently of DNA synthesis. Gene Ther. **8:**1248–1254.
17. **Miao, C. H., H. Nakai, A. R. Thompson, T. A. Storm, W. Chiu, R. O. Snyder, and M. A. Kay.** 2000. Inclusion of the hepatic locus control region, an intron, and untranslated region increases and stabilizes human factor IX gene expression in vivo, but not in vitro. Mol. Ther. **1:**522–532.
18. **Miao, C. H., H. Nakai, A. R. Thompson, T. A. Storm, W. Chiu, R. O. Snyder, and M. A. Kay.** 2000. Nonrandom transduction of recombinant adeno-associated virus vectors in mouse hepatocytes in vivo: cell cycling does not influence hepatocyte transduction. J. Virol. **74:**3793–3803.
19. **Nakai, H., R. W. Herzog, J. N. Hagstrom, J. Walter, S. H. Kung, E. Y. Yang, S. J. Tai, Y. Iwaki, G. J. Kurtzman, K. J. Fisher, P. Colosi, L. B. Couto, and K. A. High.** 1998. Adeno-associated viral vector-mediated gene transfer of human blood coagulation factor IX into mouse liver. Blood **91:**4600–4607.
20. **Nakai, H., Y. Iwaki, M. A. Kay, and L. B. Couto.** 1999. Isolation of recombinant adeno-associated virus vector-cellular junctions from mouse liver. J. Virol. **73:**5438–5447.
21. **Nakai, H., T. A. Storm, and M. A. Kay.** 2000. Increasing the size of rAAV-mediated expression cassettes in vivo by intermolecular joining of two complementary vectors. Nat. Biotechnol. **18:**527–532.
22. **Nakai, H., T. A. Storm, and M. A. Kay.** 2000. Recruitment of single-stranded recombinant adeno-associated virus vector genomes and intermolecular recombination are responsible for stable transduction of liver in vivo. J. Virol. **74:**9451–9463.
23. **Nakai, H., C. E. Thomas, T. A. Storm, S. Fuess, S. Powell, J. F. Wright, and M. A. Kay.** 2002. A limited number of transducible hepatocytes restricts a wide-range linear vector dose response in recombinant adeno-associated virus-mediated liver transduction. J. Virol. **76:**11343–11349.
24. **Nakai, H., S. R. Yant, T. A. Storm, S. Fuess, L. Meuse, and M. A. Kay.** 2001. Extrachromosomal recombinant adeno-associated virus vector genomes are primarily responsible for stable liver transduction in vivo. J. Virol. **75:**6969–6976.
25. **Qing, K., J. Hansen, K. A. Weigel-Kelley, M. Tan, S. Zhou, and A. Srivastava.** 2001. Adeno-associated virus type 2-mediated gene transfer: role of cellular FKBP52 protein in transgene expression. J. Virol. **75:**8968–8976.
26. **Qing, K., W. Li, L. Zhong, M. Tan, J. Hansen, K. A. Weigel-Kelley, L. Chen, M. C. Yoder, and A. Srivastava.** 2003. Adeno-associated virus type 2-mediated gene transfer: role of cellular T-cell protein tyrosine phosphatase in transgene expression in established cell lines in vitro and transgenic mice in vivo. J. Virol. **77:**2741–2746.
27. **Rabinowitz, J. E., F. Rolling, C. Li, H. Conrath, W. Xiao, X. Xiao, and R. J. Samulski.** 2002. Cross-packaging of a single adeno-associated virus (AAV) type 2 vector genome into multiple AAV serotypes enables transduction with broad specificity. J. Virol. **76:**791–801.
28. **Sanlioglu, S., P. K. Benson, J. Yang, E. M. Atkinson, T. Reynolds, and J. F. Engelhardt.** 2000. Endocytosis and nuclear trafficking of adeno-associated virus type 2 are controlled by rac1 and phosphatidylinositol-3 kinase activation. J. Virol. **74:**9184–9196.
29. **Scallan, C. D., D. Lillicrap, H. Jiang, X. Qian, S. L. Patarroyo-White, A. E. Parker, T. Liu, J. Vargas, D. Nagy, S. K. Powell, J. F. Wright, P. V. Turner, S. J. Tinlin, S. E. Webster, A. McClelland, and L. B. Couto.** 2003. Sustained phenotypic correction of canine hemophilia A using an adeno-associated viral vector. Blood **102:**2031–2037.
30. **Seisenberger, G., M. U. Ried, T. Endress, H. Buning, M. Hallek, and C. Brauchle.** 2001. Real-time single-molecule imaging of the infection pathway of an adeno-associated virus. Science **294:**1929–1932.
31. **Wagner, J. A., A. H. Messner, M. L. Morgan, R. Daifuku, K. Kouyama, J. K. Desch, S. Manley, A. M. Norbash, C. K. Conrad, S. Frieborg, T. Reynolds, W. B. Guggino, R. B. Moss, B. J. Carter, J. J. Wine, T. R. Flotte, and P. Gardner.** 1999. Safety and biological efficacy of an adeno-associated virus vector-cystic fibrosis transmembrane regulator (AAV-CFTR) in the cystic fibrosis maxillary sinus. Laryngoscope **109:**266–274.
32. **Xiao, W., K. H. Warrington, Jr., P. Hearing, J. Hughes, and N. Muzyczka.** 2002. Adenovirus-facilitated nuclear translocation of adeno-associated virus type 2. J. Virol. **76:**11505–11517.
33. **Xiao, W., S. C. Berta, M. M. Lu, A. D. Moscioni, J. Tazelaar, and J. M. Wilson.** 1998. Adeno-associated virus as a vector for liver-directed gene therapy. J. Virol. **72:**10222–10226.
34. **Yan, Z., R. Zak, G. W. Luxton, T. C. Ritchie, U. Bantel-Schaal, and J. F. Engelhardt.** 2002. Ubiquitination of both adeno-associated virus type 2 and 5 capsid proteins affects the transduction efficiency of recombinant vectors. J. Virol. **76:**2043–2053.